Diversity Combining Considerations for Incoherent Frequency Hopping Multiple Access Systems

Ching P. Hung and Yu T. Su, *Member, IEEE*

***Abstract*— This paper studies the problem of diversity combining for frequency-hopped multiple access (FHMA) systems that operate in a mobile satellite environment characterized by frequency-nonselective Rician multipath fading. The modulation scheme considered is the incoherent M-ary frequency-shift keying (MFSK). The optimal diversity combining rule is derived under the assumptions that the number of active users (K) in the system is known, all users are chip (hop)-synchronous, and each user employs a random FH address. We suggest practical implementations that are close approximations of the optimal rule and examine the effects of various system parameters on the resulting receivers. The bit error probability performance is analyzed and numerical examples are provided. The effects of the diversity order (L), the signaling size (M) and unequal received powers are examined and related system design concerns such as system capacity and spectral efficiency are evaluated as well.**

I. Introduction

FREQUENCY-HOPPED multiple access (FHMA) techniques have attracted considerable interests over the past two decades [1]–[13]. Cooper and Nettleton [1] first proposed an FHMA system with differential phase shift-keyed (DPSK) signaling for mobile communication applications. At about the same time Viterbi [3] initiated the use of MFSK for low-rate multiple access (MA) mobile satellite systems. Performance of FHMA/DPSK and MFSK systems in Rayleigh fading channels was analyzed by Yue [5], [6]. Using the same Rayleigh fading assumption, Goodman *et al.* [4] studied the system capability of a fast FHMA/MFSK system with a hard-limited diversity combining receiver. Bounds and approximations for the bit error probability of an asynchronous slow FHMA system with memoryless random hopping pattern were obtained by Geraniotis and Pursley [7]. The effect of unequal user power levels was analyzed by Geraniotis [8]. Assuming Markov hopping pattern, Cheun and Stark [9] analyzed the performance of both synchronous and asynchronous slow FHMA systems with BFSK signaling. Agusti [10] used a numerical integration method to evaluate the performance of both slow and fast asynchronous FHMA/BFSK communications. Recently, Fiebig [11] evaluated the spectrum efficiencies of various fast FHMA/MFSK systems; Yegani and McGillem [12] investigated the performance of a new hard-limited FHMA/MFSK system with a two-level modulation in typical factory environments (Rayleigh, Rician or lognormal fading). An FHMA/MFSK system with multi-user detection and cochannel interference cancellation is proposed by Mabuchi *et al.* [13], [14]. [8]- [11] studied additive white Gaussian noise (AWGN) channels while others considered fading environments.

When used in a mobile communication environment, a communication signal suffers not only thermal noise perturbation but also multipath fading and MA interference from other system users. MFSK signaling is employed so that the MA interference can be lessened. The diversity technique is known to be an effective measure in combating the fading effect, if an appropriate signal combining scheme is used. Yue [5] derived optimal diversity combining rules for incoherent and differentially coherent synchronous FHMA systems in the presence of nonselective Rayleigh fading. He also compared the union bound error-rate performance of three diversity combining schemes, namely, the soft-limited, hard-limited, and linear diversity combining rules. In this paper, we derive an incoherent maximum likelihood (ML) diversity combiner for FHMA/MFSK systems. The communication channel is assumed to be nonselective Rician fading, which is an appropriate model for mobile satellite channels when a line-of-sight path exists between a satellite and a mobile terminal [16]. Since the resulting nonlinearity is difficult to implement, we propose three practical receivers and analyze their performance. The rest of this paper is organized as follows. The optimal ML FHMA/MFSK diversity combining rule is derived in the next section. This part is an extension of Yue's work [5]. The influence of the channel characteristic (the Rice factor and the number of active users in the system) on the optimal nonlinearity is investigated. Three suboptimal receivers that replace the soft-limiter-like nonlinearity with a multi-level quantizer are then proposed. One of them uses an adaptive upper threshold while the other two use fixed thresholds. Hard-limited linear combiner can be regarded as a special case of these proposed combiners. Section III presents performance analysis of these suboptimal receivers. Section IV provides numerical results for the proposed receivers and discusses the capacity and spectral efficiency issues. Finally, we draw some concluding remarks in Section V. To ease the task of performance analysis we assume that the signals received by different channels at the same hopping interval

Manuscript received January 15, 1994; revised September 20, 1994. This work was supported in part by the National Science Council of Taiwan under Contract 84-2612-E-009-003.

C. P. Hung is with the Institute of Electronics, National Chiao Tung University, Hsinchu, Taiwan.

Y. T. Su is with the Department of Communication Engineering, National Chiao Tung University, Hsinchu, Taiwan.

IEEE Log Number 9407512.

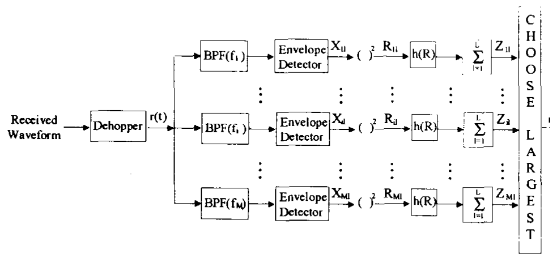

Fig. 1. Receiver block diagram of a fast FHMA/MFSK system.

are mutually independent. The Appendix examines the effect of such an approximation.

II. System Structure and Parameters

Consider the FHMA/MFSK system shown in Fig. 1. The binary data sequence of rate R_b is converted into an MFSK signal sequence of rate R_s, where $R_s = R_b/k = 1/T_s$, $k = \log_2 M$. The carrier frequency of an MFSK symbol is then hopped for L times within T_s seconds, i.e., in the subsymbol (chip) interval $(l-1)T_c < t \le lT_c$, where $T_c = 1/R_c = T_s/L$, the transmitted signal for the kth user is given by

$$\sqrt{2E_c/T_c}p(t - lT_c)\cos(2\pi f_{k_l}t + \phi_{k_l})$$

where E_c is the signal energy per chip and is assumed to be the same for all users of the system, $p(t)$ is a rectangular function of unit amplitude and is nonzero only if $0 \le t \le T_c$, and ϕ_{k_l} is the carrier phase. The transmitted carrier frequencies in a symbol time $(f_{k_0}, f_{k_1}, \cdots, f_{k_{L-1}})$ depend on both the k-bit input data and the 'address' (hopping pattern) assigned to the kth user. Let $(f_0, f_0 + W) = B$ be the frequency band available to the FHMA system and R_c be the bandwidth per channel. The total channel number is then given by

$$N = \lfloor W/R_c \rfloor = \lfloor Wk/(LR_b) \rfloor \tag{1}$$

where $\lfloor x \rfloor$ is the largest integer smaller than x and N is usually greater than M. In the system proposed in [4], $M = N$. There are several other possible frequency structures for FHMA/MFSK systems [12], [14], [15]. For example, W may be partitioned into $q = N/M$ adjacent, non-overlapping M-ary bands, each with bandwidth $M\Delta f$. To mitigate multipath fading, it is required that the chip interval $T_c = 1/R_c$ be smaller than the channel's coherent time τ_c and two adjacent channels be separated by at least a coherence bandwidth B_c. These two requirements along with the need to minimize adjacent channel interference often necessitates that $\Delta f = \tilde{n}R_c$, $\tilde{n} \ge 1$. For convenience, we shall use $\tilde{n} = 1$ in our computations and assume that no adjacent channel interference results. The numerical results so obtained can easily be converted to the more practical case $\tilde{n} > 1$ by modifying related system parameters.

An address can be an L-tuple $\mathbf{a} = (a_0, a_1, \cdots, a_{L-1})$, where $a_i \in S_h$, $S_h = \{1, 2, \cdots, q\}$ and each integer is associated with a pre-designated channel within B. The actual transmitted frequency f_{k_l} during the lth chip interval can be the mth tone of the a_ith M-ary band—$f_0 + (m-1)\Delta f + (a_i - 1)M\Delta f$—where m is determined by a k-bit data vector. The frequencies associated with an address $\mathbf{a}$ can also be allowed to be any one of the N candidate channels within the transmitting band B [3]–[5]. We shall assume that each user is given a random address, i.e., a_i is selected from a legitimate set such that each element of that set is equally likely to be chosen. The resulting performance can be regarded as the average performance over all possible users' address assignments. An suitably designed address set will certainly yield performance superior to the average performance obtained herein. As in [5], we define the following set of orthogonal basis functions which spans the band B over the interval $[0, T_s)$

$$r_{nl}(t) = \sqrt{E_c/T_c}p(t - lT_c)e^{i2\pi(f_0+n\Delta f)t}, \quad n = 1, 2, \cdots, M; l = 1, 2, \cdots, L, \tag{2}$$

where $i \overset{def}{=} \sqrt{-1}$. The transmitted signal during the symbol period $(0, T_s)$ is thus given by

$$s(t) = \sum_{l=1}^{L}\sum_{n=1}^{N} c_{nl}r_{nl}(t) \tag{3}$$

where c_{nl} is 1 or 0 and, for a given l, only one of $\{c_{nl}\}$ is nonzero. When transmitted through a frequency-nonselective slow Rician fading MA channel, the received dehopped signal is composed of three components

$$r(t) = \hat{s}(t) + I(t) + z(t) \tag{4a}$$

where $\hat{s}(t)$ is the desired signal, $I(t) = \sum_{j=1}^{J} I_j(t)$ is the interference from J other simultaneous users in the same system, and $z(t)$ is a white Gaussian noise process. The desired signal can be written as

$$\hat{s}(t) = \sum_{l=1}^{L}\sum_{n=1}^{N} \alpha_l \tilde{c}_{nl}e^{i\phi_{nl}}r_{nl}(t) \tag{4b}$$

where ϕ_{nl} are phase shifts, $\tilde{c}_{nl} = \delta_{nm}$, for some m, δ_{mn} being the Kronecker detla, and $\{\alpha_l\}$ are independent and identically distributed (i.i.d.) Rician random variables with mean a and variance $2\sigma_f^2$. Note that a^2 represents the average power of the unfaded (direct) component of the transmitted signal, and 2 σ_f^2 represents the average power of the diffused component. Equation (4b) implies that these two parameters and therefore the total average transmitted signal power per hop, $E_c = a^2 + 2\sigma_f^2$, are the same for all the L hops associated with an MFSK symbol. Defining Γ as the power ratio of the direct component and the diffused component and applying the normalization, $a^2 + 2\sigma_f^2 = 1$, we then have $a^2 = \Gamma/(1 + \Gamma)$ and 2 $\sigma_f^2 = 1/(1 + \Gamma)$, respectively. It can easily be seen that $\Gamma = 0$ is equivalent to Rayleigh fading while $\Gamma = \infty$ represents the AWGN-only case. All J interferers, like the desired signal, experience i.i.d. Rician fading, therefore, the total interference can be written as

$$I(t) = \sum_{j=1}^{J}\sum_{l=1}^{L} \tilde{\alpha}_{jl} \sum_{n=1}^{N} \tilde{c}_{jnl}e^{i\theta_{jnl}}r_{nl}(t) \tag{4c}$$

where $\tilde{\alpha}_{jl}$'s are i.i.d. Rician random variables with the common mean a and variance $\gamma^2 = \sigma_f^2$, θ_{jnl}'s are i.i.d. random variables that are uniformly distributed within $(0, 2\pi]$ and, for a given (j, l), only one $\tilde{c}_{jnl}$ is nonzero and equal to one. This interference model is a result of four assumptions. Firstly, each user has an independent random address. Secondly, within a given chip (hop) interval, all N candidate transmitting channels can be modeled as i.i.d. Rician fading channels and channel statistics at different hops are i.i.d. as well (chip-independence assumption). Thirdly, the system has exercised a power-control scheme such that none of the users in the MA network dominates and that in a noiseless environment all the signals arrive at a receiver with the same strength. Finally, all the users are chip-synchronous (but not symbol-synchronous). Note that it have shown [9]–[10] that chip-asynchronous FHMA systems perform better than their chip-synchronous counterparts.

A. Optimal Diversity Combining Rule

Let us assume that the mth bin of the M-ary signaling band is the channel so that, for all l, $\tilde{c}_{nl}$ is equal to 1 if $n = m$, and 0 otherwise. In this case, the nth energy detector output from the lth diversity branch R_{nl} (see Fig. 1) is the squared value of the complex variable U_{nl} defined by

$$U_{nl} = \alpha_l \delta_{mn} e^{i\phi_{ml}} + \sum_{j=1}^{J} \tilde{\alpha}_{jl} \tilde{c}_{jnl} e^{i\theta_{jnl}} + z_{nl} \qquad (5)$$

where z_{nl} is a zero-mean complex Gaussian random variable whose real and imaginary parts have the same variance $\sigma_0^2 \stackrel{def}{=} N_0/2$. It can be shown [17] that the characteristic function of $X_{nl} \stackrel{def}{=} |U_{nl}|$, conditioned on $\{\tilde{\alpha}_{jl}, \alpha_l, \tilde{c}_{jnl}\}$, is given by

$$\Phi_X(\lambda|\tilde{c}_{jnl}, \tilde{\alpha}_{jl}, \alpha_l) = e^{-\sigma_0^2\lambda^2/2} J_0(\alpha_l \delta_{mn}\lambda) \prod_{j=1}^{J} J_0(\tilde{c}_{jnl}\tilde{\alpha}_{jl}\lambda). \qquad (6)$$

Using the random independent hopping pattern assumption and taking the expectation with respect to $\tilde{c}_{jnl}$, we obtain

$$\Phi_X(\lambda|\tilde{\alpha}_{jl}, \alpha_l) = e^{-\sigma_0^2\lambda^2/2} J_0(\alpha_l\delta_{mn}\lambda) \prod_{j=1}^{J} [(1 - \mu + \mu J_0(\tilde{a}_{jl}\lambda)]. \qquad (7)$$

Averaging (6) with respect to $\tilde{\alpha}_{jl}$ and α_l and using the identity

$$\int_0^\infty \frac{\alpha_l}{\sigma_0} e^{-(\alpha_l^2 a)/\sigma_0^2} I_0(\frac{\alpha_l a}{\sigma^2}) J_0(\alpha_l\lambda) d\alpha_l = e^{-\sigma_0^2\lambda^2/2} J_0(a) \qquad (8)$$

we obtain

$$\Phi_{X_{nl}}(\lambda) = e^{-\frac{\lambda^2\sigma_0^2}{2}} e^{-\frac{\lambda^2\delta_{mn}}{4(1+\Gamma)}} J_0(a\lambda\delta_{mn}) \times \sum_{k=0}^{J} B(k; J, \mu) e^{-\frac{k\lambda^2\gamma^2}{2}} J_0^k(a\lambda) \qquad (9)$$

where $B(k; J, \mu) \stackrel{def}{=} \binom{J}{k}\mu^k(1-\mu)^{J-k}$ and $\mu = 1/N$. The above equation indicates that, as a result of the chip-independence assumption, the characteristic function is independent of l. We will henceforth omit the diversity parameter l in our notations whenever there is no danger of ambiguity. The corresponding probability density function (pdf) for X_{nl} can be derived from

$$f_{X_n}(x) = x \int_0^\infty \lambda J_0(x\lambda) \Phi_{X_n}(\lambda) d\lambda. \qquad (10)$$

Substituting (9) into (10) and using the transformation $R_{nl} = X_{nl}^2$, we find that the pdf of the nth energy detector output, given that the desired signal is in the mth channel, is

$$P_n(r|m) = \frac{1}{2}\int_0^\infty \lambda J_0(\sqrt{r}\lambda) \Phi_{X_n}(\lambda) d\lambda. \qquad (11)$$

For the Rayleigh fading case ($\Gamma = 0$), (11) becomes

$$P_n(r|m) = \sum_{k=0}^{J} \frac{B(k; J; \mu)}{k + 2\sigma_0^2 + \delta_{mn}} \exp\left[-r/(k + 2\sigma_0^2 + \delta_{mn})\right] \qquad (12)$$

which is the same as that obtained in [5]. In case there is no interference, (11) is reduced to (13), at the bottom of this page.

The energy detector outputs $\{R_{nl}, n = 1, 2 \cdots, M; l = 1, 2, \cdots, L\} \stackrel{\triangle}{=} \mathbf{R}$ constitute a sufficient statistic for maximum likelihood detection of incoherent MFSK signals. Strictly speaking, for a fixed l, $\{R_{nl}\}$ are not independent because the number of interferers is finite. But when $N \gg 1$ and $J \gg 1$ the bin-independence assumption (i.e., $\mathbf{R}$ are statistically independent) is considered as a valid approximation model [5]–[6], [11]–[12]. Such an approximation also leads to a simpler receiver structure, for if the correlation among $\{R_{nl}\}$ is taken into account, the resulting optimal receiver has to process mutichannel outputs simultaneously and it will have a connection complexity $O(LM^2)$. The bin-independence and the chip-independence assumptions then enable us to decompose the conditional joint pdf of $\{R_{nl}\}$

$$\Pr\left[\{R_{nl}\}|m\right] = \prod_{n=0}^{M-1}\prod_{l=1}^{L} P_{nl}(R_{nl}|m). \qquad (14)$$

A diversity combiner (demodulator) is a decision rule that, based on the observed $\mathbf{R}$, decides which tone is the correct

$$\begin{aligned} P_n(r|m) &= \frac{1}{2}\int_0^\infty \lambda J_0(\sqrt{r}\lambda) \exp\left[-\frac{\sigma_0^2 + \sigma_f^2\delta_{mn}}{2}\lambda^2\right] J_0(\sqrt{\Gamma/(1+\Gamma)}\lambda\delta_{mn}) d\lambda \\ &= \frac{1}{2(\sigma_0^2 + \sigma_f^2\delta_{mn})} \exp\left[-\frac{r + a^2\delta_{mn}}{2(\sigma_0^2 + \sigma_f^2\delta_{mn})}\right] I_0\left(\frac{\sqrt{r}a\delta_{mn}}{\sigma_0^2 + \sigma_f^2\delta_{mn}}\right) \end{aligned} \qquad (13)$$

(transmitted) signal. If the *a priori* probability that mth bin was transmitted, $p(m)$, is independent of m, then the optimal Bayses decision rule is:

Accept the hypotheses that the mth tone was transmitted (H_m) if

$$\Pr\left[\{R_{nl}\}|m\right] \geq \Pr\left[\{R_{nl}\}|k\right], \qquad \text{for all } k \neq m.$$

The fact that $P_n(R_{nl}|m) = P_n(R_{nl}|k)$, for $n \neq m \neq k$ leads to the equivalent test:

Accept H_m if

$$\sum_{l=1}^{L} \ell n\left\{P_m(R_{ml}|m)/P_m(R_{ml}|k)\right\} \geq \sum_{l=1}^{L} \ell n\left\{P_k(R_{kl}|k)/P_k(R_{kl}|m)\right\}, \forall k \neq m. \quad (15)$$

Therefore, the optimum diversity combining rule can be realized by three consecutive steps: i) let the energy detector outputs **R** pass through a common nonlinearity $g(\cdot)$, ii) add up the outputs corresponding to the same bin at different hopping intervals

$$Z_n = \sum_{l=1}^{L} g(R_{nl}) \quad (16)$$

where

$$g(R) \overset{def}{=} \ell n P_m(R|m) - \ell n P_m(R|k)$$

and then iii) decide that the kth bin was sent if $Z_k = \max_{\text{all } n} Z_n$.

B. Numerical Behavior and Suboptimal Nonlinearities

For the convenience of comparison, the optimal nonlinearity is normalized to

$$h(R) = \frac{g(R_{1/2})[g(R) - g(0)]}{g(R_{1/2}) - g(0)}, \qquad 0 < R < \infty \quad (17)$$

where $R_{1/2}$ is such that $g(R_{1/2}) = 0.5g(R_{sat})$ and the saturation input is defined by $R_{sat} = min\{R : g'(R) = 0\}$. Because the R_{sat} so defined is often difficult to locate we choose $R(20) \overset{def}{=} 20N_0$ as the reference point and redefine $R_{1/2}$ as the input value such that $g(R_{1/2}) = g(R(20))/2$. When no other user is present, i.e., $J = 0$, the optimal receiver becomes a linear diversity combiner, which is a well-known result [18]. The behavior of the normalized optimal nonlinearity $h(R)/N_0$ as a function of the Rice factor Γ of the fading channel, the number of active users J, and the normalized energy detector output R/N_0 is depicted in Fig. 2(a) and (b). Only the case $B = 20$ MHz, $R_b = 32.895$ KHz, $M = 256$, and $L = 16$ is shown but the basic shape of the optimal nonlinearity remains unaltered for other cases of interest. A common feature is that the optimal nonlinearity can be well-approximated by the soft-limiter

$$h_{sl}(R) = \begin{cases} R, & 0 < R \leq \Upsilon \\ \Upsilon, & \Upsilon < R < \infty. \end{cases} \quad (18)$$

Such a soft-limiter is much easier to implement than the optimal nonlinearity. In practice, however, the baseband demodulator is often realized in finite-precision arithmetic. In that case, the soft-limiter must be approximated by a quantizer. Since the threshold of the soft-limiter depends on the number of active users, the corresponding upper limit of the quantizer should be made adaptive. We shall refer to the receiver with an adaptive quantization threshold as a receiver of class A, or simply Receiver A. There is still a problem associated with the selection of the upper limit because the upper part of an optimal nonlinearity is not totally flat. An optimal upper limit can be found only after a case-by-case numerical search. Numerical examples indicate that it causes negligible degradation when the threshold $\Upsilon_a \triangleq h(R(20))$ is used. Although it is reasonable to assume that the number of active users $K = J + 1$ in an MA system is perfectly known. Receiver A can still be simplified if the perfect side information assumption is removed. Consider two such non-adaptive receivers which set their quantizer's upper limit to

$$\Upsilon_b \overset{def}{=} h(R(20))|_{K=N}$$

and

$$\Upsilon_c \overset{def}{=} h(R(20))|_{K=N/2}$$

respectively. The one with the fixed threshold Υ_b will be referred to as Receiver B, and the other one with Υ_c will be called as Receiver C in subsequent discussions.

III. Performance Analysis

To evaluate the performance of the receivers proposed in the previous section, let us assume, as before, that the first bin of the M-ary signaling band is the correct dehopped message bin. Then the pdfs of the quadratic detector output **R** can be derived from (11) with $m = 1$, i.e.

$$f_n(R_{nl}|m = 1) = \frac{1}{2}\int_0^\infty \lambda J_0(\lambda\sqrt{R_{nl}/\sigma_0^2})\Phi_{nl}(\lambda)d\lambda \quad (19)$$

where (20), at the bottom of this page, where $\rho \overset{def}{=} a^2/2\sigma_0^2$ and $\zeta \overset{def}{=} \sigma_f^2/\sigma_0^2$, are the signal-to-noise ratio of the direct and the diffused components, respectively. If a Q-level uniform quantizer with step size $s = \Upsilon/(Q-1)$ is used, the probability mass function (pmf) of the quantizer's outputs $\{Z_{kl} \overset{def}{=}$

$$\Phi_{kl}(\lambda) = \exp\left[-\frac{(1+\zeta\delta_{1k})\lambda^2}{2}\right] J_0(\sqrt{2\rho}\lambda\delta_{1k}) \sum_{j=0}^{J} B(j; J, \mu) J_0^j(\sqrt{2\rho}\lambda) \exp(-j\zeta\lambda^2/4) \quad (20)$$

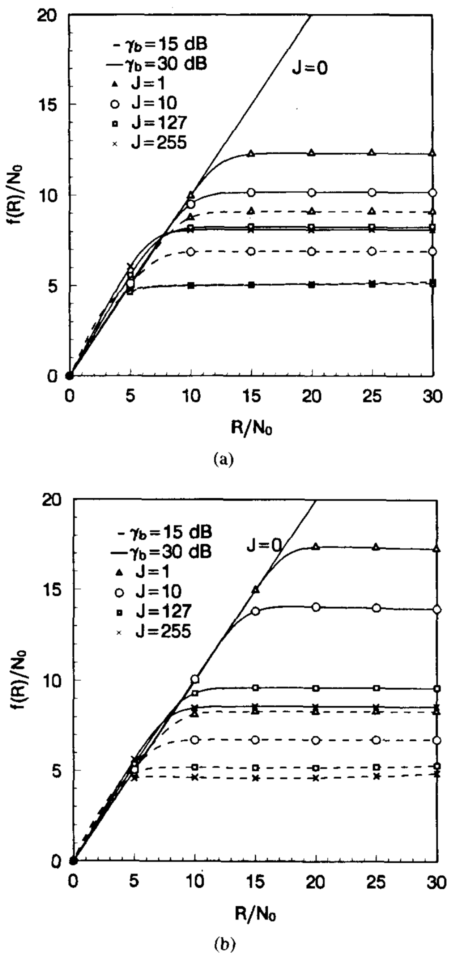

Fig. 2. Optimal nonlinearity for fast FHMA/MFSK system over Rician fading channel with $M = 256$, $L = 16$. (a) $\Gamma = 1$. (b) $\Gamma = 10$.

$h_{sl}(R_{kl}), k = 1, 2, \cdots, M, l = 1, 2, \cdots, L\}$, for the kth bin at the lth hop can be expressed as

$$\Pr[Z_{kl} = z] = P_Z(z) = \sum_{n=0}^{Q-1} V_{kl}(n)\delta(z - ns) \tag{21}$$

where

$$\begin{aligned} V_{kl}(n) &= \Pr\left\{Z_{kl} = ns\right\} \\ &= \Pr\left\{ns \le R_{kl} < (n+1)s\right\}. \end{aligned} \tag{22}$$

Therefore, for the message bin we have

$$V_{1l}(n) = \begin{cases} F_{R_{1l}}((n+1)s) - F_{R_{1l}}(ns), & n = 0, 1, \cdots, Q-2 \\ 1 - F_{R_{1l}}(\Upsilon) & n = Q-1 \end{cases} \tag{23}$$

and for other bins (i.e., $k > 1$)

$$V_{kl}(n) = \begin{cases} F_{R_{kl}}((n+1)s) - F_{R_{kl}}(ns), & n = 0, 1, \cdots, Q-2 \\ 1 - F_{R_{kl}}(\Upsilon) & n = Q-1 \end{cases} \tag{24}$$

where the cumulative distribution function is to be calculated from

$$F_{R_{kl}}(r) = \sqrt{r}\int_0^\infty J_1(\sqrt{r}\lambda)\Phi_{kl}(\lambda)d\lambda \tag{25}$$

and the characteristic function $\Phi_{kl}(\lambda)$ is defined by (20). The pmf of the diversity combiner output of the kth bin, $Z_k \overset{def}{=} \sum_{l=1}^{L} Z_{kl}$, can be obtained by an $L-$fold convolution of the single diversity pmf (21)

$$\begin{aligned} \Pr[Z_k = z] &= \left[\sum_{n=0}^{Q-1} V_{kl}(n)\delta(z - ns)\right]^{\otimes L} \\ &\overset{def}{=} \sum_{n=0}^{L(Q-1)} C_{kL}(n)\delta(z - ns) \end{aligned} \tag{26}$$

where $\otimes L$ denotes the $L-$fold convolution. The discrete probabilities $\{C_{kl}(n)\}$ can be computed recursively via

$$C_{kL}(n) = \sum_{m=m_1}^{m_2} C_{k,L-1}(n - m)V_{kL}(m) \tag{27}$$

where $m_1 = \max[0, n - (L-1)(Q-1)]$, $m_2 = \min(n, Q-1)$ and $C_{k1}(n) = V_{k1}(n)$. Using these results we can evaluate the symbol error probability $P_s(M, L)$ as follows. Note that

$$\mathrm{P}_s(M; L) = 1 - \Pr\left[\text{correct symbol decision}\right] \tag{28}$$

and

$$\begin{aligned} \Pr\left[\text{correct decision}\right] = &\Pr\left[Z_1 = \max_k Z_k\right] \\ &+ \frac{1}{2}\Pr\left[Z_1 \text{ is one of two largest } Z_k\right] \\ &+ \frac{1}{3}\Pr\left[Z_1 \text{ is one of three largest } Z_k\right] \\ &\vdots \\ &+ \frac{1}{M}\Pr\left[\text{all } Z_k \text{ are equal}\right]. \end{aligned} \tag{29}$$

The above expression is resulted from the assumption that if two or more outputs are equal, an unbiased randomized decision is to be made. After some algebra, (29) can be simplified to (30), shown at the bottom of the next page. Substituting (30) into (28) and using the relation between the bit-error probability and the symbol error probability for orthogonal M-ary signaling, we then obtain the probability of bit error. When $J = 0$ (23) and (24) can be simplified to (31), at the bottom of the page, and for $i \neq 1$

$$V_{il}(n) = \begin{cases} \exp\left\{-\frac{ns}{2\sigma_0^2}\right\} - \exp\left\{-\frac{(n+1)s}{2\sigma_0^2}\right\}, & n < Q-1 \\ \exp\left\{-\frac{\Upsilon}{2\sigma_0^2}\right\}, & n = Q-1 \end{cases} \tag{32}$$

where $Q(a,b)$ is the Marcum's Q-function defined by

$$Q(a,b) = \int_b^\infty e^{-\frac{a^2+x^2}{2}} I_0(ax)dx.$$

To compute the performance of other proposed receivers we can just replace Υ with the associated thresholds and substitute the new step sizes into (23)–(30). The hard-limited combiners belong to a special class of our investigation, $Q = 2$. The resulting error probability, however, can be expressed in a more compact form [4], [12], [14].

IV. Results and Discussions

Numerical behavior of the proposed fast FHMA/MFSK receivers is presented in this section. Throughout this section the parameters $W = 20$ MHz and $R_b = 32.895$ KHz are assumed. Define the average bit signal-to-noise ratio, γ_b as $E\left[\frac{E_b}{N_0}\alpha\right] = E(\alpha)E_b/N_0$, where α is the Rician random variable characterizing the slow fading effect of the channel. Fig. 3(a) and (b) depict the influence of the number of quantization levels used when $M = 256$, $L = 16$. These curves reveal that increasing the number of the quantization levels beyond 8 will not bring noticeable improvement. A 16-level uniform quantizer is thus used to approximate the optimal nonlinearity in the remaining numerical examples. Fig. 4(a) and (b) show bit-error rate (BER) performance of three receivers with $M = 256$, parameterized by γ_b and Γ. All three receivers yield almost identical performance in most cases. This means the system performance is not sensitive to the threshold setting so long as it is greater than a certain reasonable value. All these figures indicate that receiver A

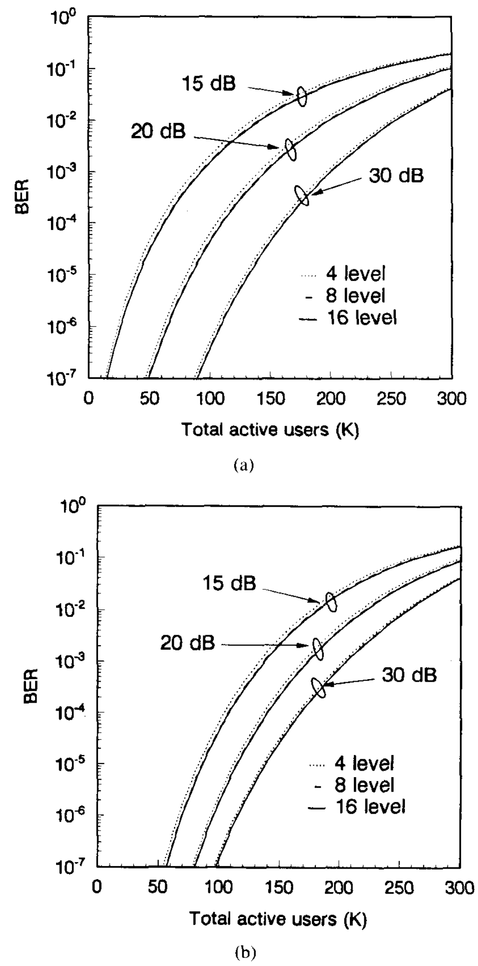

Fig. 3. BER performance of FHMA/MFSK system with Q-level quantizer ($M = 256$, $L = 16$). (a) $\Gamma = 1$. (b) $\Gamma = 10$.

$$\begin{aligned} \Pr\Big[\text{correct decision}\Big] &= \sum_{n=1}^{L(Q-1)} C_{1L}(n) \sum_{m=0}^{M-1} \binom{M-1}{m} \frac{1}{m+1} \Big\{\Pr[Z_2 = ns]\Big\}^m \\ &\quad \Big\{\sum_{k=0}^{n-1} \Pr[Z_3 = ks]\Big\}^{M-m-1} + \frac{1}{M}\Pr[Z_1 = 0]\Big\{\Pr[Z_2 = 0]\Big\}^{M-1} \\ &= \sum_{n=1}^{L(Q-1)} C_{1L}(n) \sum_{m=0}^{M-1} \binom{M-1}{m} \frac{[C_{2L}(n)]^m}{m+1} \\ &\quad \Big\{\sum_{k=0}^{n-1} C_{3L}(k)\Big\}^{M-m-1} + \frac{C_{1L}(0)}{M}\Big\{C_{2L}(0)\Big\}^{M-1} \end{aligned} \tag{30}$$

$$V_{1l}(n) = \begin{cases} Q\left(\sqrt{\frac{2\rho}{1+\zeta}}, \sqrt{\frac{ns}{\sigma_0^2(1+\zeta)}}\right) - Q\left(\sqrt{\frac{2\rho}{1+\zeta}}, \sqrt{\frac{(n+1)s}{\sigma_0^2(1+\zeta)}}\right), & n < Q-1 \\ Q\left(\sqrt{\frac{2\rho}{1+\zeta}}, \sqrt{\frac{\Upsilon}{\sigma_0^2(1+\zeta)}}\right), & n = Q-1 \end{cases} \tag{31}$$

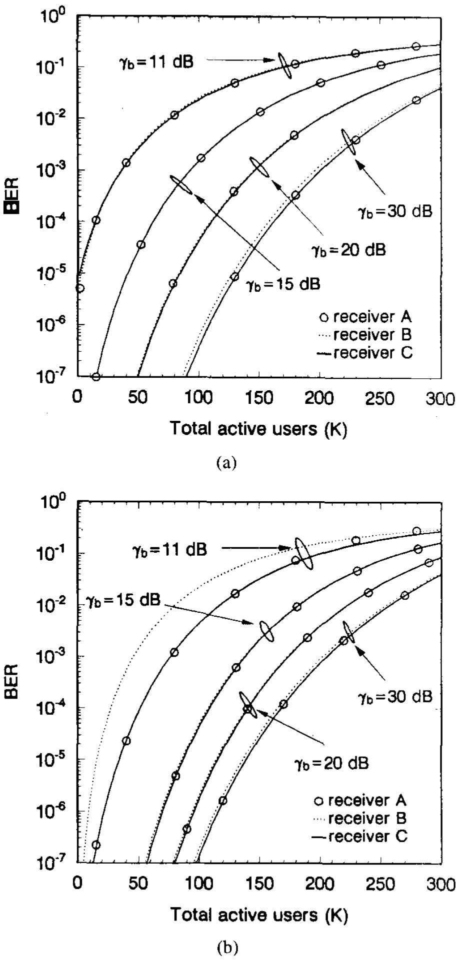

Fig. 4. BER performance of FHMA/MFSK systems with different soft-limited combining receivers ($M = 256$, $L = 16$). (a) $\Gamma = 1$. (b) $\Gamma = 10$.

has the best performance, which is expected, since it uses an adaptive threshold derived from its perfect knowledge about $K = J + 1$. Receiver C, which uses a threshold that is optimal when the $K = N/2$, is better than Receiver B and its performance is very close to Receiver A. Receiver B is the worst, especially when both γ_b and Γ are small. This may, in part, due to the fact that the optimal nonlinearity associated with Receiver B is 'more nonlinear', as can be seen from Fig. 2(a) and (b) where the deviation from the linear case $J = 0$ increases as the number of interferers increases.

As have been demonstrated by the above figures, FHMA systems are interference-limited. When a system satisfies a basic signal-to-noise requirement its performance is only limited by the number of interferers. Hence two related important performance indices are of interest to us. One is the system capacity defined as the maximum number of simultaneous active users $K_{\max}$ such that the resulting error probability is less than a predetermined specification. If the required bit-error probability is 10^{-3}, Fig. 4(a) and (b) tell us that all three receivers render almost identical system capacity in most

TABLE I
SPECTRAL EFFICIENCY AND THE ASSOCIATED SYSTEM PARAMETERS

γ_b (dB)	M	L_{opt}	k_{max}	Γ	η (%)
15	8	17	19	1	3.1
15	16	15	32	1	5.3
15	32	15	44	1	7.2
15	64	15	63	1	10.4
15	128	18	73(81)	1	12.0(13.3)
15	256	15	71(92)	1	11.7(15.1)
15	512	10	63(89)	1	10.4(14.6)
15	8	7	52	10	8.6
15	16	8	73	10	12.0
15	32	9	90	10	14.8
15	64	10	104	10	17.1
15	128	11	116(135)	10	19.1(22.2)
15	256	12	128(145)	10	21.1(23.8)
15	512	10	134(153)	10	22.0(25.2)
30	8	10	100	1	16.5
30	16	11	124	1	20.4
30	32	12	144	1	23.7
30	64	13	161	1	26.5
30	128	15	175(186)	1	28.8(30.6)
30	256	16	188(200)	1	30.9(32.9)
30	512	10	181(211)	1	29.8(34.7)
30	8	10	106	10	17.4
30	16	11	131	10	21.6
30	32	12	152	10	25.0
30	64	13	170	10	28.0
30	128	13	185(191)	10	30.4(31.4)
30	256	15	198(204)	10	32.6(33.6)
30	512	10	194(199)	10	31.9(32.7)

cases. To simplify our presentation we use Receiver C as the representative receiver in the following discussion. Fig. 5(a) shows the impacts of the parameters M, Γ and γ_b on the hard-limited FHMA/MFSK system's capacity $K_{\max}$. Both the threshold, η_t, and the diversity order, L, have been optimized. Maximum capacity is achieved by using a relatively large M ($M = 2^k$ $k \geq 7$), which is also true for soft-limited combiners, as is evidenced from Table I. The corresponding optimal diversity order, L_{opt}, is between 10 and 15 for $\Gamma = 10$ and becomes 16 or 18 when $\Gamma = 1$.

Another performance index of interest is the spectral efficiency, η, measured in number of bits per second per Hz and defined by $\eta = K_{\max} R_b / W$, where R_b is the data rate. Substituting the identity $R_b \log_2(M) = LR_c$, we have [11]

$$\eta = \frac{K_{\max} \log_2(M)}{NL} \approx \frac{K_{max} R_b}{W} \tag{33}$$

The above equation points out that the optimal diversity order L_{opt} that maximizes K also results in the largest η if W/R_b is fixed. Spectral efficiencies correspond to the systems shown in Fig. 5(a) are depicted in Fig. 5(b) and listed in Table I. Both hard-limited and soft-limited (in parentheses) cases are considered. When $\gamma_b = 15$ dB, the maximum spectral efficiency is 15.1% for $\Gamma = 1$ and 25.2% for $\Gamma = 10$. When $\gamma_b = 30$ dB, the maximum spectral efficiency is increased to 34.7% for $\Gamma = 1$ and 33.6% for $\Gamma = 10$. The enhancement achieved by using soft-limiters is around 1% $\sim$ 4.9%. In other words, the simple hard-limited combiner can suppress most of the cochannel interference a multi-level quantizer is

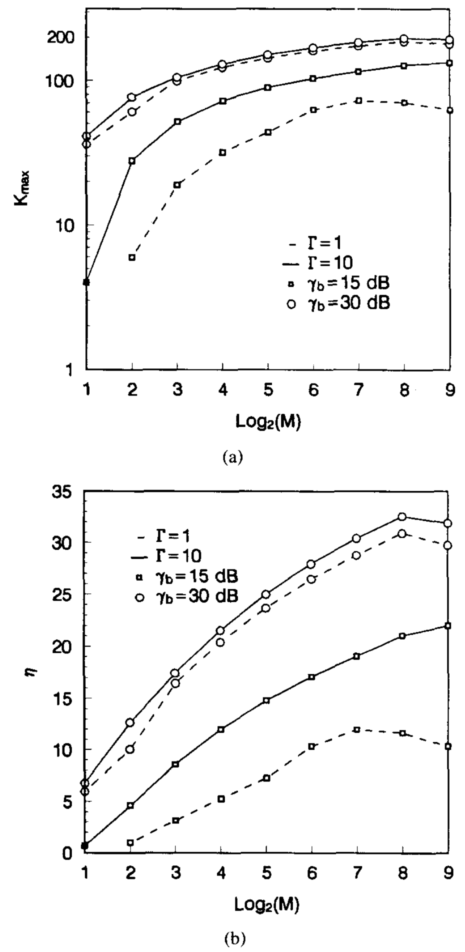

Fig. 5. Performance of the hard-limited combining receiver. (a) System capacity. (b) Spectral efficiency.

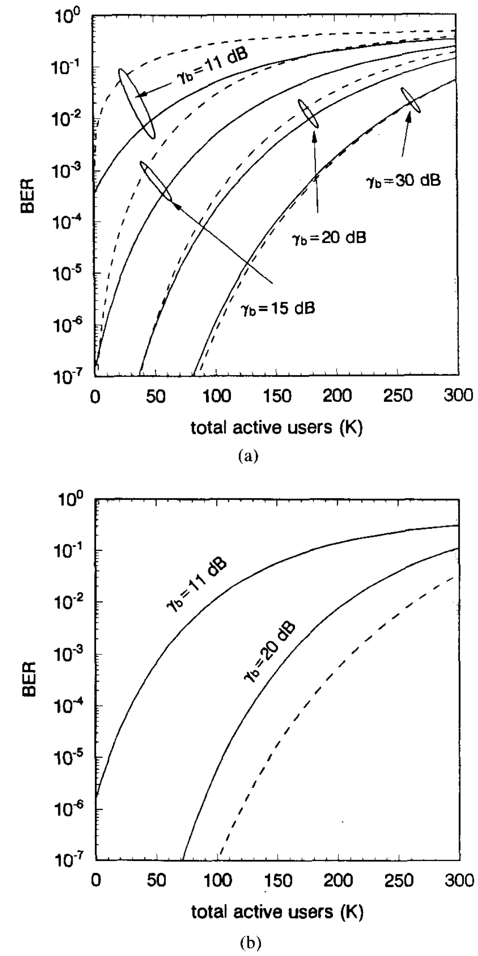

Fig. 6. BER performance comparisons ($M = 256$, $L = 16$). (a) $\Gamma = 1$. (b) $\Gamma = 10$. Solid curves are evaluated by the proposed method and dash curves are obtained by the simplified method.

expected to eliminate. System performance depends not only on the channel characteristic but also on the number of active user numbers. The influence of the former is most apparent when the average signal-to-noise ratio is low, say 15 dB. But for high γ_b, the influence of K becomes dominant, i.e., the FHMA channel becomes an interference-limited channel. Fig. 6(a) and (b) present the BER performance of hard-limited FHMA/MFSK systems in two different channels. Also shown there (dashed curves) is the performance derived from the simplified analysis method which assumes no interferer in the message bin and computes the probability of the event $\{R_{ij} > \eta_t | i \text{ is not the message bin}\}$, denoted by p_I, through [4], [12], [14]

$$p_I = p + p_F - p \cdot p_F \tag{34}$$

where

$$\begin{aligned} p &= [1-(1-1/N)^J](1-p_D), \\ p_D &= \Pr[R_{ij} > \eta_t |\ i \text{ is the message bin, no interferer}], \\ p_F &= \Pr[R_{ij} > \eta_t |\ i \text{ is not the message bin, thermal noise only}]. \end{aligned}$$

Such a simplification predicts more pessimistic results for small Γ and small to median γ_b, and shows little or no influence of γ_b when the Rice factor is not small [see the dashed curve in Fig. 6(b)]. More BER performances comparisons between hard-limited and soft-limited combiners are shown in Fig. 7(a) and (b). As expected, the soft-limited combining systems outperforms the hard-limited combining systems. The improvement of the soft-limited combiner is a decreasing function of γ_b. All the results shown so far assume a power-control mechanism is in place and all user signals arrive at the MA receiver with the same field strength. Table II shows examples of two and three unequal power levels. These results reveal that the proposed receiver structure can tolerate power level variation to some extent.

V. Conclusions

An optimal ML FHMA/MFSK receiver for frequency-nonselective slow Rician fading channels is derived and practical realizations are suggested. The corresponding BER performance is analyzed and numerical examples are given. Related

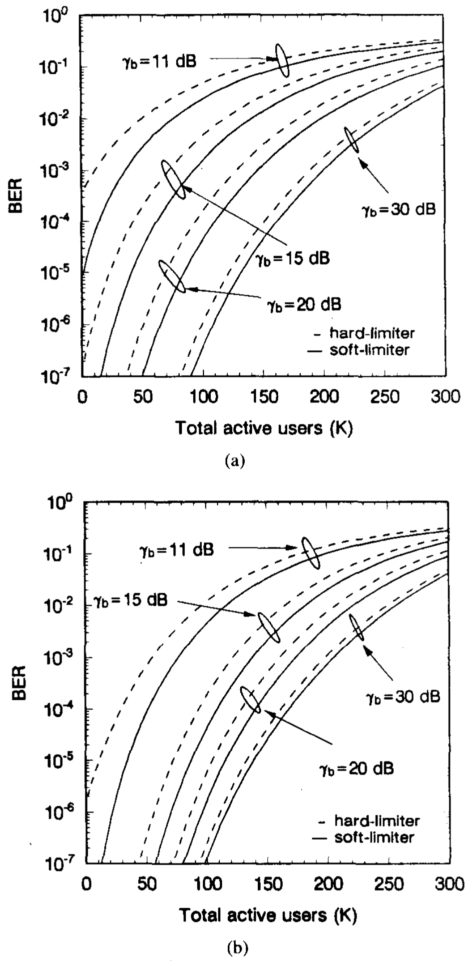

Fig. 7. BER performance of FHMA/MFSK systems for hard-limited and soft-limited combining techniques ($M = 256$, $L = 16$). (a) $\Gamma = 1$. (b) $\Gamma = 10$.

design concerns such as system capacity and spectral efficiency are evaluated. The analysis presented in this paper can be applied to systems with or without power control though we deal almost exclusively with equal power systems. Only very limited unequal power cases are examined. The results, nevertheless, indicate that the proposed receiver is not very sensitive to the power variation of the received waveforms. All the numerical results shown assume that the minimum channel spacing $\Delta f = R_c$ is used. The actual channel spacing depends on the rms delay spread of the channel used, the required chip rate and the maximum adjacent channel interference allowed. Therefore, the achievable spectral efficiency has to be divided by the factor $\tilde{\eta}$. On the other hand, the system performance can be improved by using a chip-asynchronous system with a good address assignment scheme [20], [21].

APPENDIX
EXACT BER ANALYSIS FOR BFSK SIGNALING

Let J_l be the number of interferers hitting the (dehopped) signaling band during the lth hop interval and J_{kl} be that hitting the kth bin of the signaling band. Suppose the first bin of the signaling band is the message bin then (5) can be rewritten as

$$U_{nl} = \alpha_l \delta_{1n} e^{-j\phi_l} + \sum_{j=1}^{J_l} \tilde{\alpha}_{jl} A(d, b_{jl}) e^{i\theta_{jnl}} + z_{nl}, \qquad n = 1, 2 \tag{A.1}$$

where d and b_{jl} are the message bits of the sender and the lth hop's jth interferer, $A(d, b_{il}) = \delta_{db_{il}}$ is the indicator of the (conditional) event that both the sender and the lth interferer transmit the same message bit provided that their dehopped carriers lie in the same signaling band. Let the set $\{0, 1, \cdots, Q-1\}$ be denoted I_Q and Y_l be the difference of the Q-level uniform quantizer's outputs at the lth hop, i.e., $Y_l \overset{def}{=} h(R_{1l}) - h(R_{2l})$. Then the pmf of Y_l can be expressed as

$$\Pr(Y_l = y) = \sum_{n=-(Q-1)}^{Q-1} D(n|J_l)\delta(y - ns) \tag{A.2}$$

where s is the step size of the quantizer and

$$\begin{aligned} &D(n|J_l) \\ &= \Pr[Y_l = n|J_l \text{ interferers}] \\ &= \Pr\left[\bigcup_{\substack{m-k=n \\ (m,k)\in I_Q}} \{h(R_{1l}) = ms, h(R_{2l}) = ks|J_l\}\right] \\ &= \sum_{m=\max(0,n)}^{\min(Q-1,Q-1+n)} \Pr[h(R_{1l}) = ms, h(R_{2l}) = (m-n)s|J_l] \\ &\overset{def}{=} \sum_{m=\max(0,n)}^{\min(Q-1,Q-1+n)} A_{m,m-n}. \end{aligned} \tag{A.3}$$

TABLE II
EFFECT OF UNEQUAL RECEIVED POWER LEVELS; $M = 256$, $L = 15$

E_b/N_{rm0} (dB)	Γ	power ratio	# of interferers	BER
15	1	(1,0.5)	(70,70)	0.289×10^{-1}
15	1	(1,1)	(70,70)	0.625×10^{-1}
15	1	(1,2)	(70,70)	0.993×10^{-1}
15	1	(2,0.5)	(70,70)	0.571×10^{-1}
15	1	(2,1,0.5)	(60,20,60)	0.579×10^{-1}
20	1	(1,0.5)	(70,70)	0.314×10^{-2}
20	1	(1,1)	(70,70)	0.563×10^{-2}
20	1	(1,2)	(70,70)	0.710×10^{-2}
20	1	(1,2)	(70,70)	0.418×10^{-2}
20	1	(2,1,0.5)	(60,20,60)	0.436×10^{-2}
30	1	(1,0.5)	(70,70)	0.426×10^{-4}
30	1	(1,1)	(70,70)	0.456×10^{-4}
30	1	(1,2)	(70,70)	0.456×10^{-4}
30	1	(1,2)	(70,70)	0.426×10^{-4}
30	1	(2,1,0.5)	(60,20,60)	0.430×10^{-4}
15	10	(1,1)	(70,70)	0.156×10^{-1}
15	10	(2,1,0.5)	(60,20,60)	0.974×10^{-2}
20	10	(1,1)	(70,70)	0.426×10^{-2}
20	10	(2,1,0.5)	(60,20,60)	0.165×10^{-3}
30	10	(1,1)	(70,70)	0.176×10^{-4}
30	10	(2,1,0.5)	(60,20,60)	0.146×10^{-4}

Defining $\gamma(k) = ks$ for $0 \le k \le Q-1$ and $\gamma(Q) = \infty$, we have (A.4)–(A.6), shown at the bottom of the page. Note that $\Phi_k(\lambda|\alpha_l, \alpha_{jl}, b_{jl})$, $k = 0, 1$, are the conditional characteristic functions for the message bin ($k = 1$) and noise bin ($k = 0$), respectively. Equation (A.6) can be simplified to

$$P_{jk} = \sqrt{\gamma(j)\gamma(k)} \int_0^\infty \int_0^\infty J_1(\sqrt{\gamma(j)}\lambda_1) e^{-(\sigma_0^2+\sigma_f^2)\lambda_1^2/2} J_0(a\lambda_1) \cdot J_1(\sqrt{\gamma(k)}\lambda_2) e^{-\sigma_0^2\lambda_2^2/2} I^{J_l}(\lambda_1,\lambda_2) d\lambda_1 d\lambda_2 \tag{A.7}$$

where

$$I(\lambda_1,\lambda_2) \overset{def}{=} E_{\tilde{\alpha}_{jl},b_{jl}}[J_0(\tilde{\alpha}_{jl}A(1,b_{jl})\lambda_1) J_0(\tilde{\alpha}_{jl}A(2,b_{jl})\lambda_2)] = \frac{1}{2}\Big[J_0(a\lambda_1)e^{-\sigma_f^2\lambda_1^2/2} + J_0(a\lambda_2)e^{-\sigma_f^2\lambda_2^2/2}\Big].$$

Furthermore, we can show that $P_{j0} = P_{0k} = 0$ and

$$P_{jQ} = \sqrt{\gamma(j)} \int_0^\infty J_1(\sqrt{\gamma(j)}\lambda) e^{-(\sigma_0^2+\sigma_f^2)\lambda^2/2} J_0(a\lambda) I^{J_l}(\lambda) d\lambda \tag{A.8}$$

$$P_{Qk} = \sqrt{\gamma(k)} \int_0^\infty J_1(\sqrt{\gamma(k)}\lambda) e^{-\sigma_0^2\lambda^2/2} J_0(a\lambda) I^{J_1}(\lambda) d\lambda \tag{A.9}$$

where

$$I(\lambda) = \frac{1}{2}\Big[1 + e^{-\sigma_f^2\lambda^2/2} J_0(a\lambda)\Big]. \tag{A.10}$$

The pmf of $Y \overset{def}{=} \sum_{l=1}^{L} Y_l$ is the L-fold convolution of that of Y_l

$$\Pr(Y = y) = \Big[\sum_{n=-(Q-1)}^{Q-1} D_{nl}\delta(y - ns)\Big]^{\otimes L} \overset{def}{=} \sum_{n=-L(Q-1)}^{L(Q-1)} B_{nL}\delta(y - ns). \tag{A.11}$$

The probabilities B_{nL} can be evaluated recursively

$$B_{nL} = \sum_{m=m_1}^{m_2} B_{n-m,L-1} D_{mL}$$

where $m_1 = \max[-(Q-1), n-(L-1)(Q-1)]$, $m_2 = \min(n, Q-1)$, and $B_{n1} = D_{n1}$. The conditional bit error probability $P_b(e|J_1, J_2, \cdots, J_L)$ is

$$P_b(e|J_1, J_2, \cdots, J_L) = \sum_{n=-L(Q-1)}^{-1} B_{nL} + \frac{1}{2}B_{0L}. \tag{A.12}$$

Let $J_s = \sum_{l=1}^{L} J_l$, $p_h = 2/N$, and $b(k; J, p_h) = B(k; J, p_h)/\binom{k}{J} = p_h^J(1-p_h)^{k-J}$. The unconditional bit error probability can be written as

$$\begin{aligned} P_b(M,L) &= \sum_{J_1=0}^{J} \cdots \sum_{J_L=0}^{J} \binom{J}{J_1} \cdots \binom{J}{J_L} b(JL; J_s, p_h) P_b(e|J_1, \cdots, J_L) \\ &= \sum_{\substack{\text{all } (J_1,\cdots,J_L) \\ 0 \le J_i \le J}} P(J_1, \cdots, J_L) P_b(e|J_1, \cdots, J_L). \end{aligned} \tag{A.13}$$

Since all $J!$ permutations of the interference pattern $(J_1, \cdots, J_L)$ lead to the same conditional error probability $P(e|J_1, \cdots, J_L)$, to evaluate $P_b(M, L)$, we need to compute

$$\begin{aligned} A_{jk} &= \Pr[h(R_{1l}) = js, h(R_{2l}) = ks | J_l], \\ &= E_{\alpha_l,\tilde{\alpha}_{jl},b_{jl}}[\Pr\{\gamma(j) < R_{1l} \le \gamma(j+1), \gamma(k) < R_{2l} \le \gamma(k+1) | \alpha_l, \tilde{\alpha}_{jl}, b_{jl}\}], \\ &= E_{\alpha_l,\tilde{\alpha}_{jl},b_{jl}}[\Pr\{\gamma(j) < R_{1l} \le \gamma(j+1) | \alpha_l, \tilde{\alpha}_{jl}, b_{jl}\} \Pr\{\gamma(k) < R_{2l} \le \gamma(k+1) | \alpha_l, \tilde{\alpha}_{jl}, b_{jl}\}], \\ &= P_{j+1,k+1} - P_{j,k+1} - P_{j+1,k} + P_{j,k} \end{aligned} \tag{A.4}$$

$$P_{jk} \overset{def}{=} E_{\alpha_l,\tilde{\alpha}_{jl},b_{jl}}[\Pr\{R_{1l} \le \gamma(j) | \alpha_l, \tilde{\alpha}_{jl}, b_{jl}\} \Pr\{R_{2l} \le \gamma(k) | \tilde{\alpha}_{jl}, b_{jl}\}] \tag{A.5}$$

$$= E_{\alpha_l,\tilde{\alpha}_{jl},b_{jl}} \left\{ \sqrt{\gamma(j)\gamma(k)} \int_0^\infty J_1(\sqrt{\gamma(j)}\lambda) \Phi_1(\lambda|\alpha_l, \tilde{\alpha}_{jl}, b_{jl}) d\lambda \int_0^\infty J_1(\sqrt{\gamma(k)}\lambda) \Phi_0(\lambda|\tilde{\alpha}_{jl}, b_{jl}) d\lambda \right\} \tag{A.6}$$

$$\begin{aligned} P_s(M,L) &= \sum_{J_1=0}^{J} \cdots \sum_{J_L=0}^{J} \binom{J}{J_1} \cdots \binom{J}{J_L} b(JL; J_s, M/N) P_M(e|J_1, \cdots, J_L) \\ &= \sum_{\substack{\text{all } (J_1,\cdots,J_L) \\ 0 \le J_i \le J}} P(J_1, \cdots, J_L) P_M(e|J_1, \cdots, J_L) \\ &= \sum_{J_{11}=0}^{J} \sum_{J_{12}=0}^{J} \cdots \sum_{J_{LM}=0}^{J} P(J_{11}, \cdots, J_{LM}) P_M(e|J_{11}, \cdots, J_{LM}) \end{aligned} \tag{A.16}$$

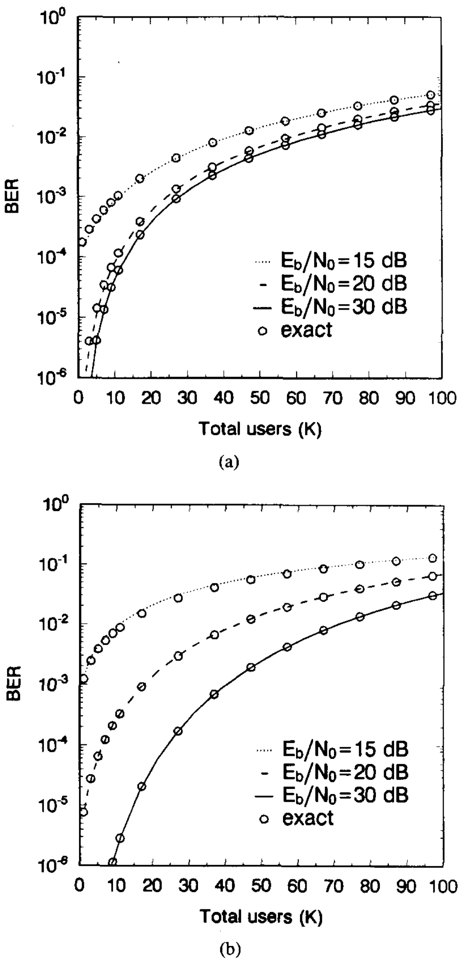

Fig. 8. BER performance of FHMA/BFSK systems: comparison of the exact analysis and the bin-independence approximation. (a) $L = 3, \Gamma = 10$. (b) $L = 6, \Gamma = 1$.

$(J+1)^L/J!$ conditional probabilities only. But this is still an enormous task when J or L is large. Note that (A.13) can also be expressed as

$$P_b(M,L) = \sum_{J_s=0}^{LJ} \sum_{\substack{(J_1,\cdots,J_L) \\ \in S(L,J_s,J)}} P(J_1,\cdots,J_L) P_b(e|J_1,\cdots,J_L)$$

$$= \sum_{J_s=0}^{LJ} P(e|J_s) \tag{A.14}$$

where $S(L,J_s,J) = \{(J_1,\cdots,J_L) : 0 \le J_i \le J, \sum_{i=1}^{L} J_i = J_s\}$, and

$$P(e|J_s) = \sum_{\substack{(J_1,\cdots,J_L) \\ \in S(L,J_s,J)}} P(J_1,\cdots,J_L) P_b(e|J_1,\cdots,J_L),$$

$$\le \sum_{\substack{(J_1,\cdots,J_L) \\ \in S(L,J_s,J)}} P(J_1,\cdots,J_L),$$

$$\stackrel{def}{=} P_u(e|J_s). \tag{A.15}$$

We have examined the behavior of $P(e|J_s)$ versus J_s for several different sets of $\{(J,L,N) : N > 100\}$ and found that in computing $P_b(e)$ via (A.14) we have to compute only a small portion of the conditional probabilities $\{P(e|J_s)\}$, even with a truncation error as small as 10^{-12}. Fig. 8(a) and (b) compare the BER performance of two FHMA/BFSK systems obtained from the approximation method and the exact analysis derived above. It is clear that the approximation is in excellent agreement with the exact analysis.

As for the MFSK case, the corresponding symbol error rate (SER) is given by (A.16), shown at the bottom of the previous page, where $P_M(e|J_1,\cdots,J_L)$ is the SER given the presence of the interference pattern $(J_1,J_2,\cdots,J_L)$ and $P_M(e|J_{11},\cdots,J_{LM})$ is that conditioned on the presence of the pattern $(J_{11},\cdots,J_{LM})$. The evaluation of the latter conditional SER can be accomplished in a way similar to what have been shown in the main text. The problem is the number of the conditional SER needed to be computed. Even with appropriate sorting of the legitimate interference patterns into equivalent classes that result in the same SER's we still have to handle a computing complexity several order larger than that of the BFSK case.

References

[1] G. R. Cooper and R. W. Nettleton, "A spread spectrum technique for high capacity mobile communication," *IEEE Trans. Veh. Technol.*, vol. VT-27, pp. 264–275, Nov. 1978.

[2] R. W. Nettleton and G. R. Cooper, "Performance of a frequency-hopped differentially modulated spread-spectrum receiver in a Rayleigh fading channel," *IEEE Trans. Veh. Technol.*, vol. VT-30, no. 1, pp. 14–29, Feb. 1981.

[3] A. J. Viterbi, "A processing-satellite transponder for multiple access by low rate mobile users," in *Proc. Digital Satellite Commun. Conf.* (Montreal, P.Q., Canada), Oct. 1978.

[4] D. J. Goodman, P. S. Henry, and V. K. Prabhu, "Frequency-hopped multilevel FSK for mobile radio," *Bell Syst. Tech. J.*, vol. 59, no. 7, pp. 1257–1275, Sept. 1980.

[5] O. C. Yue, "Maximum likelihood combining for noncoherent and differential coherent frequency-hopping multiple-access systems," *IEEE Trans. Inform. Theory*, vol. IT-28, no. 4, pp. 631–639, July 1982.

[6] ——, "Performance of frequency-hopping multiple-access multilevel FSK systems with hard-limited and linear combining," *IEEE Trans. Commun.*, vol. COM-29, no. 11, pp. 1687–1694, Nov. 1981.

[7] E. A. Geraniotis and M. B. Pursley, "Error probability for slow-frequency-hopped spread-spectrum multiple-access communications over fading channels," *IEEE Trans. Commun.*, vol. COM-30, no. 5, pp. 996–1009, May 1982.

[8] E. A. Geraniotis, "Multiple-access capability of frequency-hopped spread-spectrum revisited: An analysis of the effect of unequal power levels," *IEEE Trans. Commun.*, vol. 38, no. 7, pp. 996–1009, July 1990.

[9] K. Cheun and W. E. Stark, "Probability of error in frequency-hop spread-spectrum multiple-access communication systems with noncoherent reception," *IEEE Trans. Commun.*, vol. 39, no. 9, pp. 1400–1410, Sept. 1991.

[10] R. Agusti, "On the performance analysis of asynchronous FH-SSMA communications," *IEEE Trans. Commun.*, vol. 37, no. 5, pp. 488–499, May 1989.

[11] U. C. Fiebig, "On the efficiency of fast frequency hopping multiple-access systems," *ICC'92 Conf. Record*, July 1992, pp. 302.2.1-302.2.5.

[12] P. Yegani and C. D. McGillem "FH-MFSK multiple-access communications systems performance in the factory environment," *IEEE Trans. Veh. Technol.*, vol. 42, no. 2, pp. 148–155, May 1993.

[13] T. Mabuchi, R. Kohno, and H. Imai, "Multihopping and Decoding of Error-Correcting Code for MFSK/FH-SSMA Systems," in *Proc. IEEE Second Int. Symp. Spread Spectrum Tech., Applicat.* (Yokohama, Japan), Nov. 29–Dec. 2, 1992, pp. 199–202,

[14] ——, "Multiuser detection scheme based on canceling cochannel interference for MFSK/FH-SSMA system," *IEEE J. Select. Areas Commun.*, vol. 12, no. 4, pp. 593–604, May 1994.

[15] M. K. Simon, J. K. Omura, R. A. Scholtz, and B. K. Levitt, *Spread Spectrum Communications*, vol. II. Rockville, MD: Computer Science Press, 1985.
[16] D. Divsalar and M. K. Simon, "Trellis coded modulation for 4800-9600 bps transmission over a fading mobile satellite channel," *IEEE J. Select. Areas Commun.*, vol. SAC-5, pp. 162–175, Feb. 1987.
[17] J. S. Bird, "Error performance of binary NCFSK in the presence of multiple tone interference and system noise," *IEEE Trans. Commun.*, vol. COM-33, no. 3, pp. 203–209, Mar. 1985.
[18] J. M. Wozencraft and I. M. Jacobs, *Principle of Communications Engineering* New York: Wiley, 1967, ch. 7.
[19] I. S. Gradshteyn and I. M. Ryzhik, "Tables of integrals, series, and products," corrected and enlarged ed. New York: Academic, 1971.
[20] G. Solomon, "Optimal frequency hopping sequences for multiple access," in *Proc. 1973 Symp. Spread Spectrum Commun.* (San Diego, CA), Mar. 13–16, 1973, pp. 33–35.
[21] G. Einarsson, "Address assignment for a time-frequency-coded, spread-spectrum system," *Bell Syst. Tech. J.*, vol. 59, no. 7, pp. 1241–1255, Sept. 1980.

Ching P. Hung was born in Tainan, Taiwan, in 1961. He received the B.S. degree in electrical engineering from National Sun Yat-Sen University, Kaouhsiung, Taiwan, and the M.S. degree in communication engineering from National Chiao Tung University, Hsinchu, Taiwan, in 1984 and 1986, respectively. He is working toward the Ph.D. degree at National Chiao Tung University.

From 1988 to 1990, he was with the Telecommunication Laboratories. During this period he was engaged in MIC amplifiers and multiplier design for satellite communication. His main research interests are in the areas of spread spectrum communications and portable communication.

Yu T. Su (S'81–M'83), for a photograph and biography, please see this issue, page 221.